The EMBO Journal (2009) 28, 578–590 | © 2009 European Molecular Biology Organization | All Rights Reserved 0261-4189/09
www.embojournal.org

THE EMBO JOURNAL

Mechanisms of pre-apoptotic calreticulin exposure in immunogenic cell death

Theocharis Panaretakis[1,2,3,12], Oliver Kepp[1,2,3,12], Ulf Brockmeier[4,12], Antoine Tesniere[1,2,3], Ann-Charlotte Bjorklund[5], Daniel C Chapman[4], Michael Durchschlag[6], Nicholas Joza[1,2,3], Gérard Pierron[7], Peter van Endert[8,9], Junying Yuan[10], Laurence Zitvogel[2,3,11], Frank Madeo[6], David B Williams[4] and Guido Kroemer[1,2,3,*]

[1]INSERM, Unit 848, Villejuif, France, [2]Institut Gustave Roussy, Villejuif, France, [3]Université Paris Sud, Paris 11, Villejuif, France, [4]Department of Biochemistry, University of Toronto, Toronto, Ontario, Canada, [5]CancerCentrum Karolinska, Karolinska Institute, Stockholm, Sweden, [6]Institute of Molecular Biosciences, University of Graz, Graz, Austria, [7]CNRS, FRE 2937, Institut Andre Lwoff, Villejuif, France, [8]INSERM, U580, Paris, France, [9]Faculté de Médecine René Descartes, Université Paris-Descartes, Paris, France, [10]Department of Cell Biology, Harvard Medical School, Boston, MA, USA and [11]INSERM, U805, Institut Gustave Roussy, Villejuif, France

Dying tumour cells can elicit a potent anticancer immune response by exposing the calreticulin (CRT)/ERp57 complex on the cell surface before the cells manifest any signs of apoptosis. Here, we enumerate elements of the pathway that mediates pre-apoptotic CRT/ERp57 exposure in response to several immunogenic anticancer agents. Early activation of the endoplasmic reticulum (ER)-sessile kinase PERK leads to phosphorylation of the translation initiation factor eIF2α, followed by partial activation of caspase-8 (but not caspase-3), caspase-8-mediated cleavage of the ER protein BAP31 and conformational activation of Bax and Bak. Finally, a pool of CRT that has transited the Golgi apparatus is secreted by SNARE-dependent exocytosis. Knock-in mutation of eIF2α (to make it non-phosphorylatable) or BAP31 (to render it uncleavable), depletion of PERK, caspase-8, BAP31, Bax, Bak or SNAREs abolished CRT/ERp57 exposure induced by anthracyclines, oxaliplatin and ultraviolet C light. Depletion of PERK, caspase-8 or SNAREs had no effect on cell death induced by anthracyclines, yet abolished the immunogenicity of cell death, which could be restored by absorbing recombinant CRT to the cell surface.

The EMBO Journal (2009) **28,** 578–590. doi:10.1038/emboj.2009.1; Published online 22 January 2009
Subject Categories: differentiation & death
Keywords: calreticulin; caspase; endoplasmic reticulum stress; ERp57; exocytosis

*Corresponding author. INSERM, U848, Institut Gustave Roussy, PR1, 39, rue Camille Desmoulins, 94805 Villejuif, France.
Tel.: +33 1 42 11 60 46; Fax: +33 1 42 11 60 47;
E-mail: kroemer@igr.fr
[12]These authors contributed equally to this work

Received: 27 June 2008; accepted: 29 December 2008; published online: 22 January 2009

Introduction

Conventional anticancer treatments by radiotherapy or chemotherapy are generally thought to act through selective killing of tumour cells or by irreversibly arresting their growth. This concept focuses on the capacity of therapeutic agents to eradicate tumour cells and to spare normal cells, within a therapeutic window, yet neglects the possible contribution of the host to the elimination of malignant cells. Accumulating evidence indicates that several chemotherapeutic agents, as well as radiotherapy, are more efficient against tumours that are implanted in immunocompetent hosts than against the same tumours growing on immunodeficient mice (Casares *et al*, 2005; Apetoh *et al*, 2007; Obeid *et al*, 2007a). This has been shown for a series of mouse cancer cell lines (CT26 colon cancer, EL4 thymoma, GOS osteosarcoma, MCA205 fibrosarcoma and TS/A mammary carcinoma) that are syngeneic for different MHC backgrounds ($H2^b$ and $H2^d$), responding to a panel of distinct agents (oxaliplatin (OXP), anthracyclines or local γ-irradiation) (Casares *et al*, 2005; Apetoh *et al*, 2007; Obeid *et al*, 2007a, c). The therapeutic efficacy of anticancer agents is compromised in *rag2*$^{-/-}$ mice, which lack B and T cells, *nu/nu* mice, which lack T cells, *Ifnγ*$R^{-/-}$ mice, which cannot respond to IFN-γ, as well as in *TLR4*$^{-/-}$ mice, which cannot respond to danger signals such as HMGB1 (Apetoh *et al*, 2007). Breast cancer patients who carry a mutation in TLR4, which diminishes its interaction with HMGB1, relapse more rapidly after anthracycline chemotherapy than patients carrying the normal TLR4 allele (Apetoh *et al*, 2007), suggesting that the concept of 'immunogenic chemotherapy' also applies to humans.

Although some cytotoxic agents induce immunogenic cell death, others do not (Obeid *et al*, 2007c). When CT26 or MCA205 cells were treated with distinct chemotherapeutic agents and then evaluated for their capacity to elicit a specific immune response, it turned out that anthracyclines, OXP and ionizing irradiation (such as γ-rays and ultraviolet C (UVC) light) induced immunogenic cell death, whereas many other agents failed to do so (Obeid *et al*, 2007c). Mass spectroscopic identification of surface proteins exposed during immunogenic (as opposed to non-immunogenic) cell death led to the identification of two interacting proteins, calreticulin (CRT) and the disulphide isomerase ERp57, which appear at the surface of cells that are treated with immunogenic cell death inducers (Obeid *et al*, 2007c; Panaretakis *et al*, 2008). Both proteins are usually contained in the lumen of the endoplasmic reticulum (ER) and translocate to the cell surface within a few hours after treatment, well before the cells exhibit phosphatidylserine residues or manifest other signs of apoptosis (Obeid *et al*, 2007c; Panaretakis *et al*, 2008). Thus, the immunogenic surface exposure of the CRT/ERp57 complex involves a subtle process that is rather different from the general mixing of intracellular and plasma membranes that accompanies late-stage apoptosis (Franz *et al*, 2008;

Panaretakis *et al*, 2008). CRT apparently functions as an engulfment signal for dendritic cells (DCs). Blockade of CRT or depletion of CRT with small interfering RNAs (siRNAs) blocks the immunogenicity of cell death (Obeid *et al*, 2007c). More importantly, cells that lack ERp57 (and which hence are unable to expose CRT) become resistant against chemotherapy, not because they would fail to die in response to chemotherapeutic agents but because they fail to elicit an immune response when they die (Panaretakis *et al*, 2008).

The biomedical implications of the aforementioned notions can be summarized as follows. First, chemotherapy is only optimal when it elicits immunogenic cell death, thereby provoking an immune response that eliminates or controls residual cancer cells. Second, the inability of tumour cells to emit immunogenic signals (such as CRT exposure) may contribute to the failure of chemotherapy. Therefore, it appears important to understand the molecular pathways that are triggered by immunogenic chemotherapeutics and that lead to the translocation of endogenous CRT (endo-CRT) to the cell surface (ecto-CRT).

The pre-existing knowledge on the CRT/ERp57 exposure pathway is fragmentary, yet intriguing. Cancer cells expose CRT/ERp57 even when they are enucleated (Obeid *et al*, 2007c), meaning that the DNA damage triggered by anthracyclines, OXP or ionizing irradiation is irrelevant to the process. We found that CRT/ERp57-exposing drugs augmented ER Ca^{2+} efflux and that blockade of Ca^{2+} efflux inhibited CRT/ERp57 relocation, whereas manipulations designed to increase ER Ca^{2+} leakage facilitated CRT/ERp57 exposure (Tufi *et al*, 2008). Finally, broad-spectrum caspase inhibitors (such as Z-VAD-fmk or p35) abolish the CRT/ERp57 translocation (Obeid *et al*, 2007c), although this process occurs at a pre-apoptotic stage (Obeid *et al*, 2007c). The exact regulatory mechanisms that determine whether CRT/ERp57 is exposed or not are elusive. Moreover, the subcellular origin of CRT/ERp57 that appears on the surface, as well as the exact mode of translocation, is unknown.

On the basis of these premises, we decided to reexamine the mechanisms that regulate and mediate CRT/ERp57 exposure. As we show here, this pathway involves the sequential activation of an ER stress response, a subapoptotic caspase activation step, as well as the exocytosis of CRT/ERp57.

Results and discussion

Elements of the ER stress response are required for CRT/ERp57 exposure

Murine CT26 colon cancer cells expose CRT/ERp57 on the plasma membrane surface in response to inducers of immunogenic cell death, including the anthracycline mitoxantrone (MTX) (Obeid *et al*, 2007c; Panaretakis *et al*, 2008), OXP (Panaretakis *et al*, 2008) or UVC irradiation (Obeid *et al*, 2007a; Panaretakis *et al*, 2008), three agents that have in common the induction of reactive oxygen species (Charruyer *et al*, 2005; Laurent *et al*, 2005; Vibet *et al*, 2007). *N*-Acetyl cysteine and glutathione ethyl ester, two antioxidants, inhibited CRT/ERp57 exposure, as well as apoptosis induced by MTX, OXP or UVC (Figure 1A–C), in line with the idea that a general (rather than substance specific) stress response might trigger the CRT/ERp57 translocation to the cell surface. However, CRT exposure occurred before the cells became apoptotic and exposed annexin V on the surface (Obeid *et al*, 2007c) or lost their mitochondrial transmembrane potential (Supplementary Figure 1A–D). In addition, only CRT and ERp57 became detectable at the cell surface, whereas other ER proteins including calnexin (CNX), PDI, BIP and Grp94 remained undetectable, suggesting that CRT/Erp57 exposure is not the result of a general scrambling of cellular membranes but rather results from a specific process (Supplementary Figure 2).

MTX, OXP and UVC induced the rapid (within 4 h or less) expression of GADD34, a protein that is usually induced by ER stressors (Novoa *et al*, 2001). Moreover, MTX, OXP and UVC induced the phosphorylation of the ER stress kinase PERK on threonine 980 (Figure 1D and E), which is indicative of PERK activation (Harding *et al*, 2000). Accordingly, the PERK substrate eIF2α was phosphorylated on serine 51 (S51) (Figure 1D and E). Thapsigargin induced GADD45 expression, as well as PERK and eIF2α phosphorylation, yet failed to stimulate CRT/ERp57 exposure (Figure 1F), indicating that ER stress alone is not sufficient to mediate CRT/ERp57 translocation. The S51 phosphorylation of eIF2α is a quintessential hallmark of the ER stress response and mediates the translational arrest that is required for adaptive responses (Kaufman, 1999). Cells in which wild-type eIF2α is replaced by the non-phosphorylatable S51A mutant failed to expose CRT/ERp57 in response to MTX, OXP and UVC (Figure 1G), pointing to an essential role of the ER stress response in CRT/ERp57 exposure. Depletion of PERK (but not that of another eIF2α kinase, PKR) by transient transfection with a specific siRNA (Figure 2A) abolished the MTX-triggered CRT/ERp57 exposure (Figure 2C). In contrast, the removal of other elements of the ER stress response, ATF6 (with a siRNA) or IRE1 (by knockout) did not affect CRT exposure (Supplementary Figure 3A and B).

A stable CT26 clone expressing a PERK-specific small hairpin RNA (shRNA), in which PERK was near-to-completely depleted (clone 3 in Figure 2A), lost the capacity to phosphorylate eIF2α upon MTX treatment (Figure 2B). PERK knockdown abolished the CRT/ERp57 exposure induced by MTX, OXP or UVC (Figure 2C and D; Supplementary Figure 4A). Depletion of PERK had no effect on the induction of cell death by MTX, neither in short-term experiments (when apoptosis was measured) nor in long-term experiments (when clonogenic survival was assessed) (Supplementary Figure 4B and C), meaning that the lethal and the immunogenic response could be uncoupled at this level.

When MTX- or OXP-treated CT26 cells were injected subcutaneously into syngeneic BALB/c mice they were highly efficient in preventing the growth of live, untreated CT26 cells injected 1 week later. This vaccination effect was attenuated when wild-type CT26 cells (or a clone expressing the control SCR shRNA (shCO)) (Figure 2E) were substituted by CT26 cells depleted from PERK. This relative deficiency in immunogenicity could be reverted by absorbing recombinant CRT (recCRT) protein to the surface of PERK-deficient cells. These results confirm that CRT/ERp57 exposure has to be intact so that agents such as MTX or OXP can induce fully immunogenic cell death.

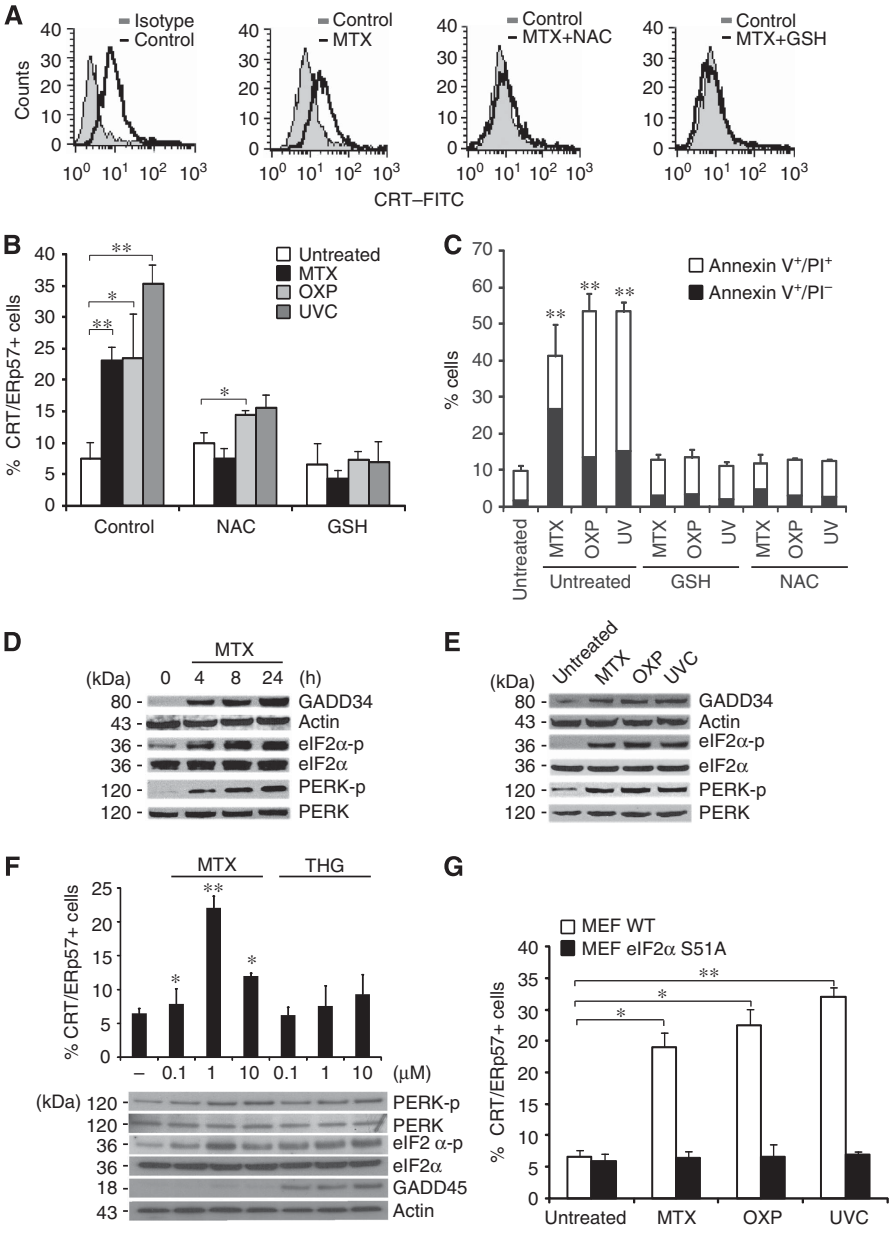

Figure 1 ROS and ER stress mediate the cell surface exposure of CRT/ERp57. (**A**) CRT/ERp57 exposure depends on ROS production. CRT/ERp57 surface exposure was analysed among viable untreated CT26 cells and in cells upon pre-incubation with NAC or GSH and/or additional treatment with MTX (for 4 h) using flow cytometry. Representative histograms are shown. (**B**) A quantitative analysis of CRT/ERp57 surface exposure was performed by analysing untreated CT26 cells or cells upon pre-incubation with NAC or GSH and/or additional treatment with MTX, OXP or UVC (for 4 h) using flow cytometry (means ± s.d., $n=3$) for the detection of CRT, $^{*}P<0.05$, $^{**}P<0.01$). (**C**) Cell death was analysed after annexin V/PI staining by flow cytometry (means ± s.d., $n=3$, $^{**}P<0.01$) at 24 h post-treatment depicting efficient protection from cell death induced by GSH and NAC. (**D**) ER stress upon treatment with CRT/ERp57-exposing stimuli. GADD34 induction, eIF2α and PERK phosphorylation were analysed in CT26 cells together with adequate loading controls upon treatment with MTX for the indicated time points (**E**) or upon treatment of CT26 cells with the indicated inducers by immunoblot. (**F**) Quantitative analysis of CRT/ERp57 surface exposure was performed by analysing CT26 cells treated with the indicated concentrations of MTX and THG for 4 h. GADD45 induction, eIF2α and PERK phosphorylation were analysed together with adequate loading controls upon treatment of CT26 with the conditions above by immunoblot. (**G**) ER stress necessary for CRT/ERp57 exposure. CRT/ERp57 surface exposure was measured by flow cytometry in untreated MEF WT and eIF2α S51A and in cells after treatment with MTX, OXP or UVC (means ± s.d., $n=3$ of CRT measurements, $^{*}P<0.05$, $^{**}P<0.01$).

Pre-apoptotic activation of apoptosis effectors is indispensable for CRT/ERp57 exposure

MTX-induced immunogenicity requires the activation of caspases that are inhibited by the modified peptide Z-VAD-fmk or by the baculovirus-encoded inhibitor of apoptosis, protein p35 (Casares *et al*, 2005). Unexpectedly, neither the ER stress-elicited caspase, caspase-12 (Nakagawa *et al*, 2000), nor the most common effector caspases-3 or -7 were involved in CRT/ERp57 exposure, because *casp12*$^{-/-}$ or *casp3*$^{-/-}$ *casp7*$^{-/-}$ mouse embryonic fibroblasts (MEFs) maintained the capacity to expose CRT/ERp57 in a Z-VAD-fmk-repressible manner (Supplementary Figure 5A). To identify the initiator caspase elicited by MTX, CT26 cells were incubated in the presence of biotinylated VAD-fmk, which was as

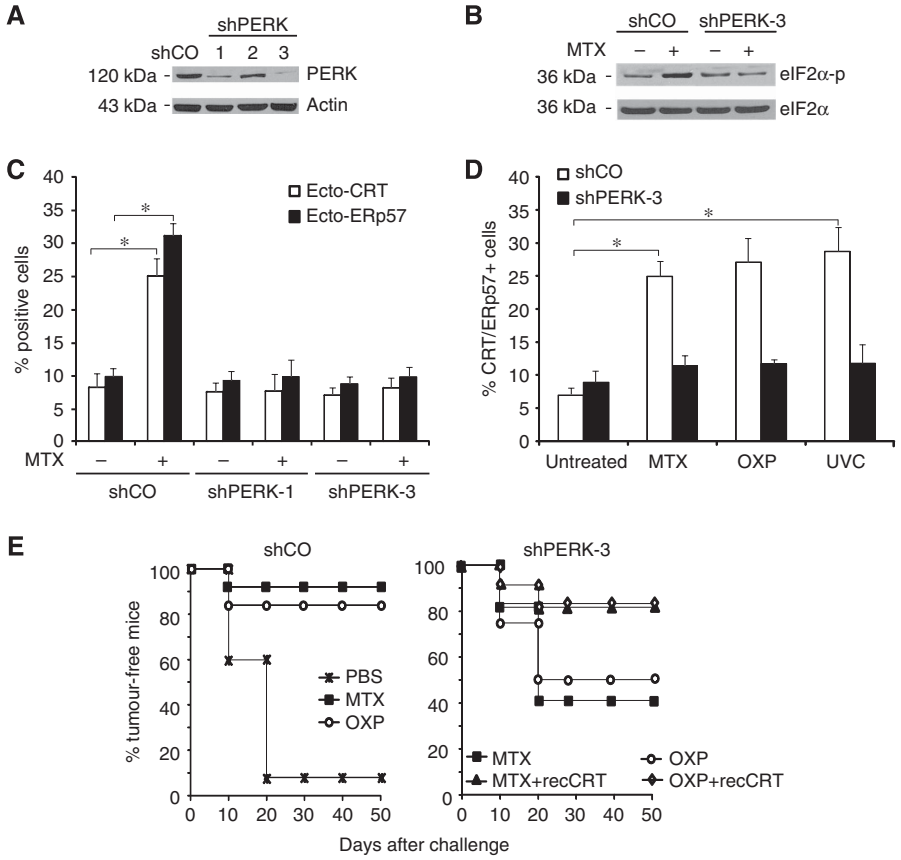

Figure 2 The ER stress kinase PERK is required for the cell surface exposure of CRT/ERp57. (**A**) PERK knockdown abolishes eIF2α phosphorylation. PERK knockdown in CT26 shPERK clones 1–3 was validated by immunoblot analysis with shCO cells used as a negative control and actin used as a loading control. (**B**) EIF2α phosphorylation was analysed in untreated CT26 shCO and shPERK clone-3 cells or treated with MTX. EIF2α was used as a loading control. (**C**) PERK is upstream of eIF2α phosphorylation and CRT/ERp57 surface exposure. CRT/ERp57 surface exposure was measured by flow cytometry in untreated and MTX-treated CT26 shCO and shPERK clones 1 and 3, (**D**) and in CT26 shCO and shPERK clone 3 upon treatment with MTX, OXP or UVC (means ± s.d., $n=3$ of ERp57 measurements,*$P<0.05$). (**E**) Vaccination effect lost upon PERK knockdown. BALB/c mice were injected with PBS control or CT26 shCO clones treated with MTX or OXP. The mice were rechallenged after 7 days with live CT26 cells (left panel) or primarily injected with CT26 shPERK clone 3 treated with MTX or OXP with optional absorption of recCRT to their surface followed by rechallenge (right panel). Subsequently, the tumour growth was monitored for the indicated times ($n=10$).

efficient in inhibiting CRT exposure as Z-VAD-fmk and p35 (Supplementary Figure 5B and C). As an enzymatic pseudo-substrate, biotinylated VAD-fmk covalently reacts with the large subunit of initiator caspases, 'trapping' the first caspase activated in a cascade (Tu *et al*, 2006). Biotinylated proteins recovered from CT26 cells treated in the presence of MTX plus biotinylated VAD-fmk contained an increasing amount of caspase-8, as early as 4 h after initiation of the experiment (Figure 3A), that is well before caspase-3 is activated (Figure 3A, left panel). Kinetic analyses revealed that MTX and OXP (but not thapsigargin) induced the proteolytic maturation of caspase-8 before that of caspase-3 (Figure 3B). Apparently, only a fraction of caspase-8 is activated at 4 h because most of caspase-8 is not yet biotinylated (Figure 3A, right panel). Caspase-8-deficient (*casp8*$^{-/-}$) MEF failed to expose CRT/ERp57 in response to MTX, OXP or UV (Figure 3C; Supplementary Figure 5D), and similar results were obtained for a CT26 clone expressing a caspase-8-depleting shRNA (shCasp8-1) (Figure 3D and E). Caspase-8 depletion did not affect cell death induction by MTX (Supplementary Figure 5E and F), yet abolished CRT/ERp57 exposure induced by MTX, OXP or UVC (Figure 3E), indicating that the pathways that lead to cell death or CRT/ERp57 exposure diverge at this level or upstream thereof. Caspase-8-depleted CT26 cells were unable to mediate tumour vaccination after MTX or OXP treatment, and this defect could be restored by absorbing recCRT protein to the surface of the cells (Figure 3F), confirming the cardinal role of caspase-8 in facilitating CRT-dependent immunogenicity.

Knockdown of PERK abolished proteolytic maturation of caspase-8 induced by MTX (Figure 4A). In contrast, *caspase 8*$^{-/-}$ MEF exhibited a normal PERK-mediated eIF2α phosphorylation (Figure 4B) supporting that PERK operates upstream of caspase-8 and not vice versa. Caspase-8 activation by addition of the death receptor ligand TRAIL induced CRT exposure. TRAIL-induced CRT exposure, not apoptosis, was inhibited by antioxidants underscoring that caspase activation is required but not sufficient for CRT exposure (Supplementary Figure 6A and B). Conversely, MTX-, OXP- or UV-induced apoptosis was not inhibited by a TRAIL-blocking antibody (Supplementary Figure 6C) or by neutralization of CD95 L (not shown), suggesting that death receptor ligands are not involved in CRT exposure. Caspase-8 was required for the degradation of its substrate Bap31 (Figure 4B), an ER-sessile protein, which has previously

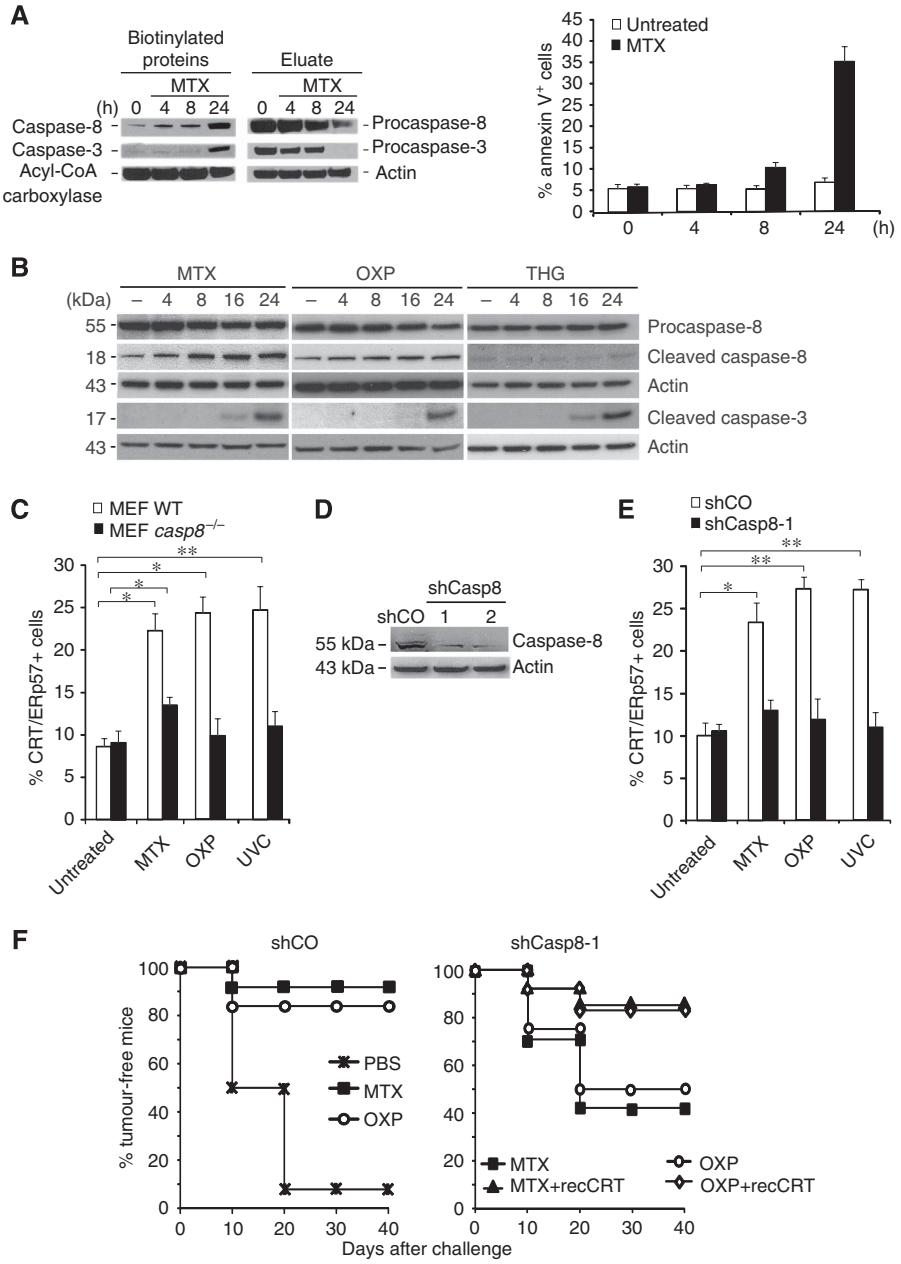

Figure 3 Caspase-8 is necessary for the cell surface exposure of CRT/ERp57. (**A**) Identification of initiator caspase by *in situ* trapping. Active and total caspase-8 and -3 were analysed in untreated HeLa and in cells treated for the indicated times with MTX. Upon *in situ* trapping with bVAD-fmk, streptavidin precipitates and eluates were analysed by immunoblot. In parallel, PS exposure was analysed by annexin V in flow cytometry (means ± s.d., $n=3$). Acyl-CoA carboxylase, which is an endogenously biotinylated protein, was detected as a loading control. (**B**) The cleavage of procaspase-8 and procaspase-3 was analysed by immunoblot in CT26 cells untreated or treated with MTX, OXP and THG for the indicated time points. Actin was used as a loading control. (**C**) Caspase-8 is necessary for CRT/ERp57 surface exposure. CRT/ERp57 surface exposure was measured by flow cytometry, in untreated MEF WT, *casp8*$^{-/-}$ and in cells treated with MTX, OXP or UVC (means ± s.d., $n=3$ of ERp57 measurements, $^{*}P<0.05$). (**D**) Loss of CRT/ERp57 surface exposure and immunogenicity in stable knockdowns of caspase-8. The knockdown of caspase-8 in CT26 shCasp8 clones 1 and 2 was analysed by immunoblot. shCO was used as a negative control and actin as a loading control. (**E**) CRT/ERp57 surface exposure was measured in untreated CT26 shCO and shCasp8 clone-1, and in cells upon treatment with MTX, OXP or UVC by flow cytometry (means ± s.d., $n=3$ of ERp57 measurements, $^{*}P<0.05$, $^{**}P<0.01$). Note that the percentage of annexin V^{+} or PI^{+} cells in the treated samples was not increased above background levels (5–10%) during the treatment with MTX, OXP or UVC for 4 h (in D, E). (**F**) Tumour growth was monitored for the indicated times in BALB/c mice injected with PBS control, or with CT26 shCO cells treated with MTX or OXP and rechallenged after 7 days with live CT26 cells (left panel) or primarily injected with CT26 shPERK clone 3 treated with MTX and OXP with optional pre-absorption of recCRT followed by rechallenge (right panel) ($n=10$).

been implicated in the lethal response to ER stress (Breckenridge *et al*, 2003). HeLa cells transfected with the uncleavable D164A/D238A Bap31 mutant (Nguyen *et al*, 2000) (Supplementary Figure 7A) lost the capacity of CRT/ERp57 translocation (Supplementary Figure 7B), and the knockdown of Bap31 similarly abrogated CRT/ERp57 exposure (Supplementary Figure 7C), suggesting that Bap31 cleavage products participate in the relocation of CRT/ERP57, perhaps as a result of increased Ca^{2+} efflux which is stimulated by the p20 fragment (Breckenridge *et al*, 2003),

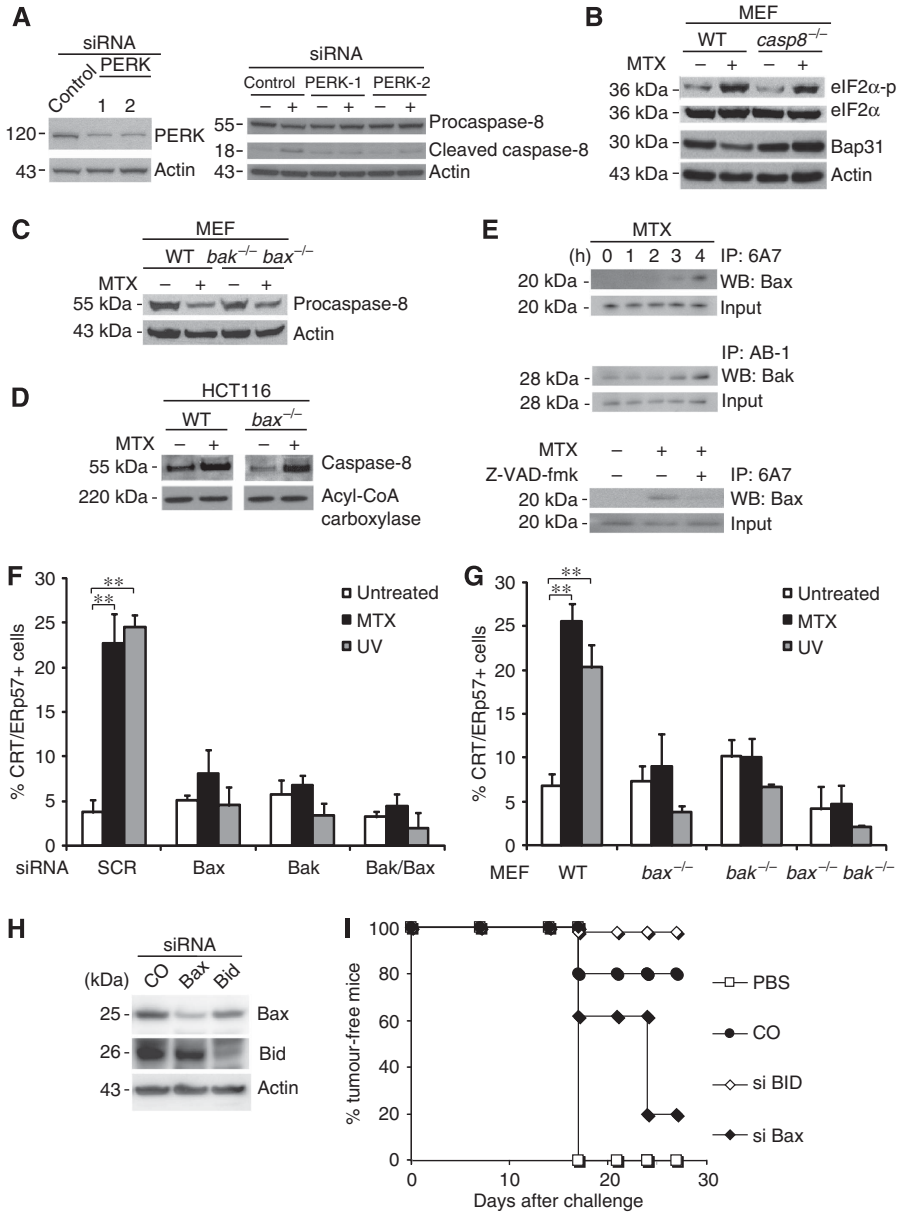

Figure 4 Pre-apoptotic activation of Bak and Bax is required for the cell surface exposure of CRT/ERp57. (**A**) ER stress precedes caspase-8 activation. Immunoblot analysis of CT26 cells transfected with either control siRNA or PERK siRNA-1 and -2 and treated with MTX for 4 h. (**B**) Immunoblot analysis of the phosphorylated levels of eIF2α and full-length Bap31 in WT and casp8$^{-/-}$ MEF cells treated with MTX. Actin was used as a loading control. (**C**) Activation of caspase-8 independent of Bax and Bak. The cleavage of pro-caspase-8 was analysed in untreated or MTX-treated WT and *bak*$^{-/-}$*bax*$^{-/-}$ MEF by immunoblot. (**D**) The activation of caspase-8 was monitored in untreated and MTX-treated WT and *bax*$^{-/-}$ HCT116 cells using bVAD-fmk followed by streptavidin precipitation. Acyl-CoA carboxylase was measured as a loading control. (**E**) Active Bax and Bak in HeLa cells treated for the indicated times with MTX (upper panels) and/or Z-VAD-fmk (lower panel) were immunoprecipitated and analysed by immunoblot. Here, 95% of the lysate was used for immunoprecipitation and 5% was used as an input control. (**F**) Activation of Bak and Bax is necessary for CRT/ERp57 exposure. The percentage of ecto-CRT/ERp57-positive cells was measured by flow cytometry in HeLa cells transfected with siBak, siBax or both after treatment with the indicated agents (means ± s.d., $n=3$ of CRT measurements, $^{**}P<0.01$). (**G**) Percentage of ecto-CRT/ERp57 in untreated WT, *bak*$^{-/-}$, *bax*$^{-/-}$ and *bak*$^{-/-}$*bax*$^{-/-}$ MEF and in cells treated with MTX was measured by flow cytometry (means ± s.d., $n=3$ of CRT measurements, $^{**}P<0.01$). (**H**) Immunoblot analysis of Bid and Bax protein levels in CT26 cells transfected with Bax and Bid siRNA, respectively. Actin was used as a loading control. (**I**) Tumour growth was monitored in BALB/c mice injected with PBS or with MTX-treated CT26 cells, which were previously transfected with siRNAs specific for Bid or Bax, 7 days before rechallenge with live CT26 cells ($n=5$).

knowing that Ca^{2+} efflux can stimulate surface exposure of CRT/ERp57 (Tufi *et al*, 2008).

As Bap31 is a Bcl-2-binding protein, we wondered whether proteins of the Bcl-2 family would affect CRT/ERp57 exposure. Indeed, we found that HeLa cells overexpressing Bcl-2 (or a cytomegalovirus-encoded protein that possesses a similar fold and function, vMIA) (Goldmacher *et al*, 1999; Pauleau *et al*, 2007) were unable to expose CRT/ERp57 in response to MTX (Supplementary Figure 7D). MEF lacking both pro-apoptotic multi-domain proteins of the Bcl-2 family, Bax and Bak, exhibited a normal MTX-triggered caspase activation, as indicated by the reduction of the inactive

caspase-8 precursor (Figure 4C). Similarly, HCT116 colon cancer cells lacking Bax exhibited a normal increase in the interaction between biotinylated VAD-fmk and caspase-8 in response to MTX (Figure 4D). Within hours after MTX addition, Bax reacted with the 6A7 antibody that specifically recognizes the N terminus of Bax, which is only exposed on active Bax, after a conformational change. This Bax activation occurred within 3–4 h, that is approximately 1 day before the cells acquired an apoptotic morphology (Supplementary Figure 7E). Both Bax and Bak adopted an active conformation within hours, and hence could be immunoprecipitated with antibodies specific for activated Bax or Bak (Figure 4E). The Bax activation was fully inhibited by the caspase inhibitor Z-VAD-fmk (Figure 4E) and PERK depletion (not shown). The knockdown of either Bax or Bak (in HeLa cells; Figure 4F) or the knockout of either Bax or Bak (in MEF; Figure 4G; Supplementary Figure 8A) abolished CRT/ERp57 exposure in response to MTX, OXP and UV. In addition, reconstitution of the expression of Bax in HCT116 cells lacking Bax led to the reappearance of CRT/ERp57 on the cell surface of cells treated with MTX (Supplementary Figure 8B). The knockdown of Bax (but not that of Bid) reduced the capacity of MTX-treated CT26 cells to mediate anticancer vaccination *in vivo* (Figure 4H and I), and this defect in immunogenicity could be restored by adsorbing recCRT to the surface of the cells.

In conclusion, MTX and other inducers of immunogenicity cause an early pre-apoptotic caspase-8 activation coupled with Bax/Bak activation, downstream of the ER stress response. Both caspase-8 and Bax/Bak are essential for CRT/ERp57 exposure and the immunogenicity of MTX-induced cell death.

Vesicular transport mechanisms leading to CRT/ERp57 exposure

As CRT has been reported to be present in cellular compartments as diverse as the ER, nucleus, cytosol, secretory granules and the plasma membrane (Bedard *et al*, 2005), it was important to determine the subcellular origin and the intracellular pathway whereby CRT is expressed at the surface of pre-apoptotic cells. Under normal circumstances, CRT is not glycosylated. On the basis of the crystal structure of the CRT paralogue CNX (Schrag *et al*, 2001), modelling studies (Kapoor *et al*, 2003), the NMR structure of the CRT arm domain (Ellgaard *et al*, 2001) and functional similarities (Leach *et al*, 2002), we introduced mutations into predicted surface-exposed segments of the CRT protein (D162N, D195N and A197T) that created two N-glycosylation sites at residues 162 and 195 (Supplementary Figure 9). This mutated haemagglutinin (HA)-tagged protein (CRT–HA) was expressed in CT26 cells, and its glycosylation state both intracellularly and

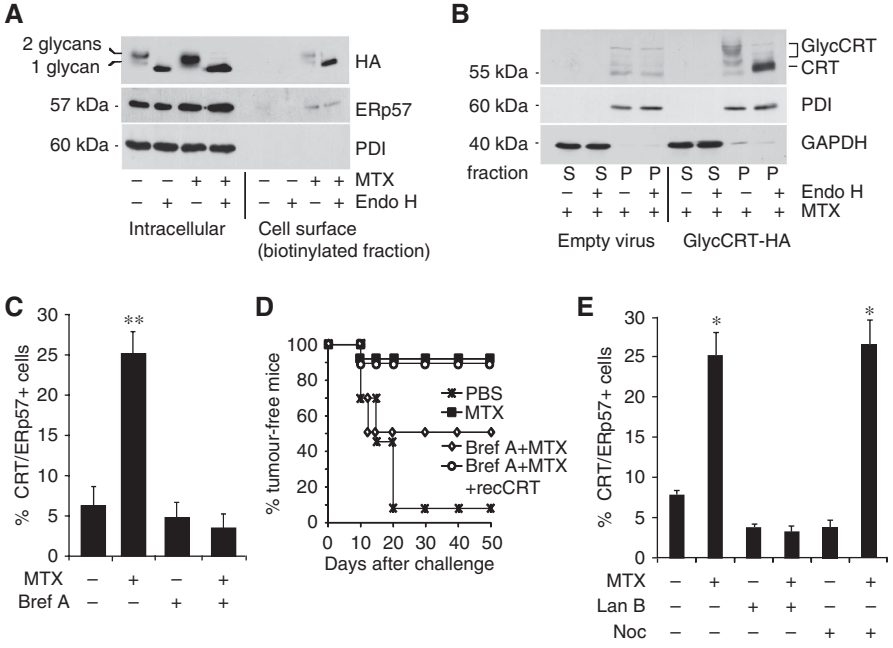

Figure 5 Ecto-CRT/ERp57 originates from the endoplasmic reticulum. (**A**) CT26 cells expressing mouse HA-tagged CRT with glycosylation sites at positions 162 and 195 were cultured in the presence or absence of MTX for 12 h. Subsequently, cells were biotinylated, lysed and incubated with streptavidin-agarose to produce a bound cell surface fraction and an unbound intracellular fraction. Fractions were digested in the presence or absence of endoglycosidase H (endo H) and analysed by immunoblotting with anti-HA mAb (to detect glycosylated CRT), anti-ERp57 and anti-PDI antisera, the latter serving as an ER marker to demonstrate the selectivity of the biotinylation procedure. A representative immunoblot is shown. (**B**) CT26 cells expressing glycosylated CRT–HA were incubated with MTX for 4 h and were permeabilized with 5 μg/ml digitonin and centrifuged to produce an organelle fraction (pellet, P) and a cytosol fraction (supernatant, S). Aliquots of the supernatant and pellet fractions corresponding to the same cell number were incubated in the absence or presence of endo H, separated by SDS–PAGE and immunoblotted with anti-HA antiserum. Blots were also re-probed with anti-glyceraldehyde 3-phosphate dehydrogenase (GAPDH) and anti-PDI as markers of the cytosol and ER lumen, respectively. A representative western blot is shown. (**C**) Anterograde ER–Golgi trafficking implicated in the CRT/ERp57 pathway. CRT/ERp57 surface exposure was measured by flow cytometry in CT26 cells pre-incubated with brefeldin A followed by MTX treatment. (means ± s.d., $n=3$ of ERp57 measurements, $^{**}P<0.01$). (**D**) Anterograde ER–Golgi trafficking necessary for immunogenicity. Tumour growth was monitored for the indicated times in BALB/c mice injected with PBS control, or with CT26 cells treated with MTX alone or MTX plus brefeldin A with optional pre-absorption with recCRT and rechallenged after 7 days with live CT26 cells ($n=10$). (**E**) CRT/ERp57 surface exposure was measured in untreated CT26 cells or in cells pre-incubated with latrunculin B (Lan B) or nocodazole (Noc) with and without MTX treatment (means ± s.d., $n=3$ of ERp57 measurements, $^{*}P<0.05$).

at the cell surface was examined by surface biotinylation. Intracellular CRT–HA appeared as two bands, which collapsed to a single species after deglycosylation with endoglycosidase H (endo H), demonstrating that the mutated CRT–HA was a mixture of singly and doubly glycosylated species (Figure 5A). Following MTX treatment, the same two glycosylated species appeared at the cell surface (ecto-CRT–HA), confirming that the ecto-CRT–HA originated in the ER, the site where N-glycosylation takes place (Figure 5A). As ecto-CRT–HA did not display the resistance to endo H digestion that often accompanies transit through the Golgi apparatus, we determined whether it trafficked through the conventional secretory pathway or through an alternative route such as retrotranslocation from ER to cytosol (Afshar *et al*, 2005). Subcellular fractionation experiments showed that glycosylated CRT–HA was present in the organelle pellet fraction with none detectable in the cytosol (Figure 5B). Furthermore, brefeldin A, an inhibitor of anterograde protein transport for the ER to the Golgi apparatus (Lippincott-Schwartz *et al*, 1989), blocked CRT/ERp57 exposure (Figure 5C; Supplementary Figure 10A and B) and annihilated the capacity of CT26 cells to vaccinate against cancer after MTX treatment (Figure 5D). In line with the role of the actin-dependent, anterograde (rather than the microtubule-dependent, retrograde) ER–Golgi traffic (Valentijn *et al*, 1999, 2000) in CRT exposure, inhibition of the actin skeleton with latrunculin B abolished CRT exposure, whereas inhibition of microtubules with nocodazole failed to do so (Figure 5E). Moreover, MTX induced a rapid reorganization of the actin cytoskeleton (Supplementary Figure 11A) and of the ER ultrastructure (Supplementary Figure 11B), but this did not alter vesicular traffic through the secretory pathway, as the rates of ER to Golgi transport of the H-2K^d molecule were unchanged in the absence or presence of drug treatment (Supplementary Figure 12).

Exocytic vesicles emanating from the Golgi have to fuse with the plasma membrane through molecular interactions between vesicle-associated SNAREs (such as VAMP1) and plasma membrane-associated SNAREs (such as SNAP23/25) (Ferro-Novick and Jahn, 1994; Rothman and Sollner, 1997). In CT26 cells, patches of ecto-CRT colocalized with dense areas of surface SNAP23 (Supplementary Figure 13A). Knockdown of VAMP1 or SNAP23 in CT26 cells (Figure 6A) abolished CRT/ERp57 exposure in response to MTX, OXP or UVC (Figure 6B; Supplementary Figure 13B). Similarly, SNAP25 depletion caused defective CRT/ERp57 exposure in HeLa cells (Supplementary Figure 14A and B). Again, blockade of exocytosis by removal of SNAP23 did not affect the

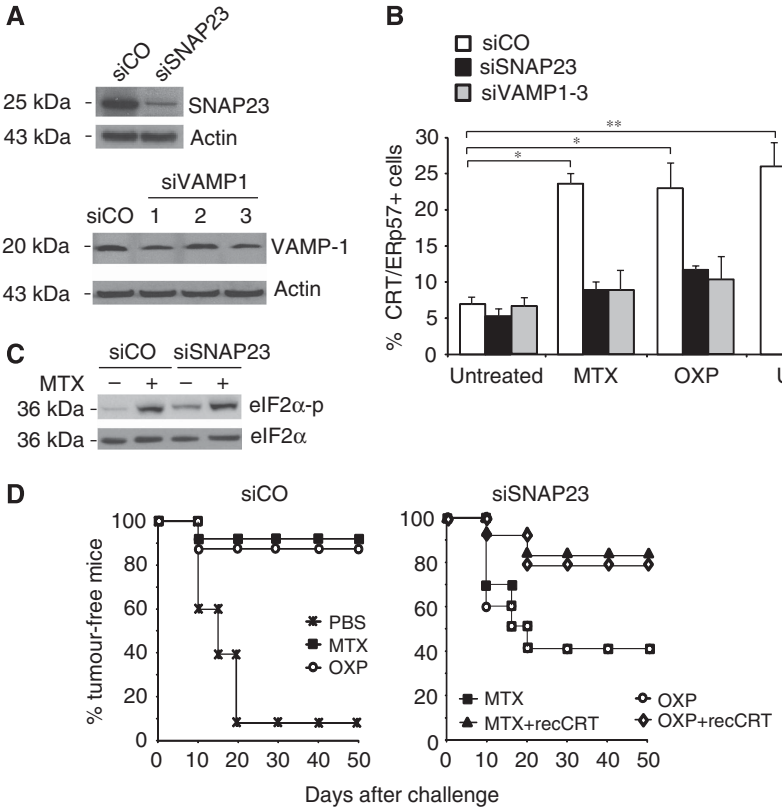

Figure 6 Ecto-CRT/ERp57 translocates to the cell surface through exocytosis. (**A**) Exocytotic vesicular transport is necessary for CRT/ERp57 exposure. Knockdown efficiency of siSNAP23 and siVAMP1 was analysed by immunoblot in transiently transfected CT26 cells. Actin was used as a loading control. (**B**) CT26 transiently transfected with siSNAP23 or siVAMP1-3 was treated with MTX, OXP or UVC and the percentage of cells showing surface exposure of CRT/ERp57 was measured by flow cytometry (means ± s.d., $n=3$ of ERp57 measurements, $^*P<0.05$). (**C**) EIF2α phosphorylation was analysed by immunoblot in untreated and MTX-treated CT26 cells transiently transfected with siSNAP23. (**D**) Importance of the exocytotic machinery for vaccination efficacy. BALB/c mice were injected with PBS control or CT26 cells transiently transfected with siCO (left panel) or siSNAP23 (right panel). The cells were left untreated or were treated with MTX or OXP and recCRT was optionally absorbed to the surface. The cells were rechallenged after 7 days with live CT26 cells and the subsequent tumour growth was monitored for the indicated times.

lethal action of MTX on CT26 cells (Supplementary Figure 15A and B) nor did it affect the MTX-induced activation of eIF2α phosphorylation (Figure 6C) or caspase-8 activation (not shown). However, blockade of SNAP23 reduced the vaccination efficacy of MTX- or OXP-treated CT26 cells, and this reduction was reversed by absorbing recCRT protein to the SNAP23-deficient cells (Figure 6D).

Altogether, these data clarify the source of ecto-CRT and the mechanisms of endo- to ecto-CRT conversion. ER-derived CRT is exocytosed through a classical, SNARE-dependent pathway that is elicited downstream of the ER stress and caspase-8/Bax/Bak activation step.

Concluding remarks

When cells are confronted with some particular stressors, such as MTX, OXP and UVC, they surface-expose CRT/ERp57, which in turn functions as an engulfment signal for DC and signals potential immunogenicity (Obeid *et al*, 2007a, b). Here, we unravel a sequence of key events that are required (but not sufficient) to transform cellular stress into this immunogenic signal (Figure 7). As a first common denominator, MTX, OXP and UVC elicit an ER stress response in which the serine/threonine kinase PERK becomes activated (as indicated by its phosphorylation) and phosphorylates eIF2α. Both the action of PERK and the phosphorylation of eIF2α are required for CRT/ERp57 exposure because depletion of PERK and non-phosphorylatable eIF2α mutant abolish CRT/ERp57 relocation. In addition, some elements of the apoptotic machinery become activated a few hours after the addition of MTX, OXP and UVC, well before the cells actually undergo apoptosis and manifest chromatin condensation, loss of the mitochondrial transmembrane potential or

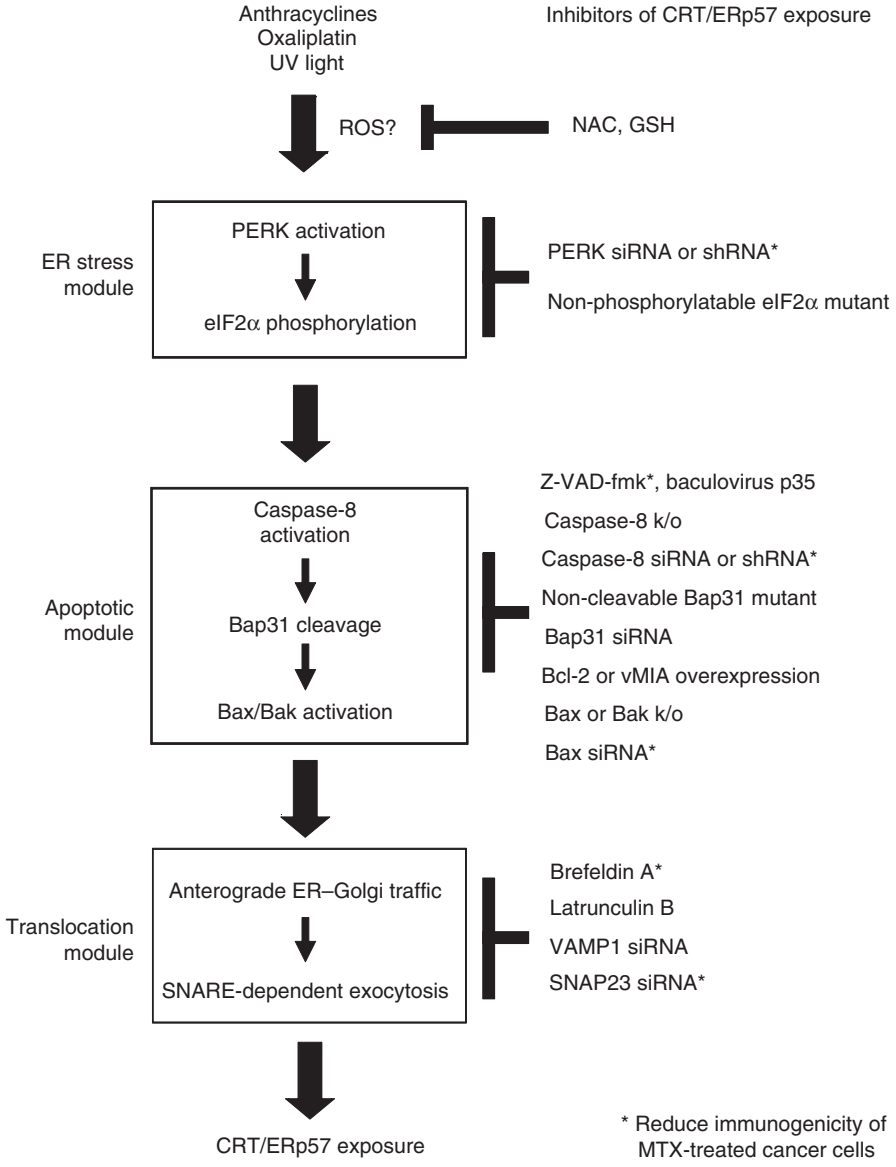

Figure 7 Hypothetical scheme of the pathway of CRT/ERp57 exposure. In response to immunogenic cell death inducers, three modules are activated, namely an ER stress module, an apoptotic module and a translocation module. The hierarchy among these modules has been established. However, the exact molecular links among them remain unclear. Moreover, the level at which ROS contributes to CRT/ERp57 exposure is elusive. The scheme lists elements of the pathway that are *necessary* for CRT/ERp57 exposure. However, the activation of these elements is not *sufficient* to induce CRT/ERp57 exposure. Inhibitors of CRT/ERp57 exposure are listed on the right. Those inhibitors that also reduce the immunogenicity of cell death *in vivo* have been marked with asterisks.

phosphatidylserine exposure. This subapoptotic event involves a partial caspase-8 (but not caspase-3) activation, as well as, downstream of caspase-8, the conformational activation of Bax and Bak. Deletion of caspase-8, Bax or Bak or inhibition of these proteins (with Z-VAD-fmk or p35 for caspases and Bcl-2 or vMIA for Bax/Bak) inhibits CRT exposure, yet does not affect the eIF2α phosphorylation, suggesting that the ER stress response occurs upstream of caspase-8, Bax and Bak. However, there is likewise an intimate relationship between the ER stress response and activation of the caspase-8/Bax/Bak module because Bap31, an ER-sessile protein that interacts with Bcl-2-like proteins (Ng *et al*, 1997), which is cleaved by caspase-8 (Breckenridge *et al*, 2003), is required for CRT/ERp57 exposure. Moreover, Bcl-2 family proteins are known to regulate Ca^{2+} fluxes on the ER membrane (Scorrano *et al*, 2003), and Ca^{2+} efflux favours ER stress responses (Schroder and Kaufman, 2005) as well as CRT/ERp57 exposure (Tufi *et al*, 2008). CRT/ERp57 appears on the surface of stressed cells as a result of exocytosis, following a classical pathway in which Golgi apparatus-derived vesicles fuse with the plasma membrane in a SNARE-dependent manner. Importantly, CRT/ERp57 exposure precedes the acquisition of hallmarks of apoptosis such as PS exposure, loss of the mitochondrial transmembrane potential and chromatin condensation. However, thus far we have not observed a single example in which CRT/ERp57 exposure could be induced without that the cells would die later, suggesting that CRT/ERp57 exposure is triggered by a level of irreversible cellular damage. In this context, it should be underscored that induction of apoptosis is usually not preceded by CRT/ERp57 exposure (Obeid *et al*, 2007c) and that only a few cell death inducers are capable of inducing immunogenic cell death. Hence, CRT/ERp57 exposure depends on the upstream signals that lead to cell death, yet is not an automatic correlate of apoptosis.

The before-mentioned linear scenario is supported by the present data, yet raises some intriguing problems. For instance, the commonly used ER stressors thapsigargin, tunicamycin and brefeldin A do not induce CRT/ERp57 exposure (Obeid *et al*, 2007c), suggesting that the type of ER stress inflicted by these agents is inadequate for the stimulation of CRT/ERp57 relocation (perhaps due to a massive ER disorganization) or that ER stress response is required but not sufficient to induce CRT/ERp57 translocation. The nature of this putative, additional signal elicited by MTX, OXP or UVC is elusive, yet must be cytoplasmic because cytoplasts (cells without nuclei) can expose CRT (Obeid *et al*, 2007c). Furthermore, it appears intriguing that the caspase-8 activation is (spatially?) limited and does not set off the entire caspase activation cascade that would lead to apoptosis. The mechanisms of this limitation are elusive. However, limited caspase-8 activation is known to participate in non-apoptotic processes such as T-cell activation, macrophage differentiation and lamellipodial assembly (Black *et al*, 2004; Kang *et al*, 2004; Ben Moshe *et al*, 2007). Antioxidants fail to inhibit TRAIL-induced (caspase-8-dependent) apoptosis, yet inhibit TRAIL-induced CRT exposure, suggesting that ROS must have some discrete function in the CRT exposure pathway. At the level of the CRT translocation machinery, two questions remain unsolved. First, it is difficult to understand that CRT/ERp57 surface exposure requires the activity of the exocytic pathway, yet an (artificial) CRT mutant bearing N-linked glycans does not receive Golgi modifications. Second, CRT is a soluble protein that can be absorbed to a saturable receptor present on the plasma membrane surface. The nature of this receptor remains elusive.

The knockdown of PERK, caspase-8, Bax or SNAP23 led to a near-to-complete abolition of CRT exposure and reduced (but did not abolish) the immunogenicity of cell death. This may either mean that the correlation between CRT exposure and immunogenicity is nonlinear (so that a minor residual exposure would be sufficient to confer some degree of immunogenicity) or that additional, yet-to-be-discovered CRT/ERp57-independent molecules can determine the switch between immunogenic and non-immunogenic cell death. On theoretical grounds, chemotherapy may fail because cancer cells do not die in response to chemotherapy. In addition, chemotherapy might fail because cell death occurs in a non-immunogenic manner, meaning that the immune system will not be alerted and cannot contribute to the fight against residual tumour cells. As shown here, the absence of several of the elements that determine immunogenicity had no effect on cell death. This kind of 'uncoupling' was observed for PERK, caspase-8 or SNAP23, the depletion of which did not affect cell death induction by MTX yet greatly reduced CRT/ERp57 exposure (*in vitro*) and immunogenicity (*in vivo*). Thus, an entirely new class of proteins that *a priori* have no impact on cell death *per se* could influence the chemotherapeutic response *in vivo*, by determining the switch between immunogenic and non-immunogenic cell death. It will be important to understand which component of the chemotherapeutic response prevails, in patients, in which particular circumstances (tumour type and treatment): cell death as such versus immunogenic cell death followed by an anticancer immune response. This kind of information might help to create algorithms in which the relative expression levels of proteins required for tumour cell death and stress-elicited immunogenic signalling can be interpreted with respect to their prognostic and predictive impact.

Materials and methods

Antibodies and reagents

The rabbit polyclonal and mouse monoclonal antibodies against CRT (ab2907 and ab22683, respectively), the rabbit polyclonal antibody against ERp57 (ab10287), the goat polyclonal antibody against GADD34 (ab9869), the rabbit polyclonal antibodies against BAP31 (ab37120), SNAP23/25 (ab50357/53723) and VAMP-1 (ab3346), acetyl-CoA carboxylase (ab63531) and the rat polyclonal against Bap31 (ab15044) were purchased from Abcam. The rabbit polyclonal antibodies against the phosphorylated form of PERK (mAB 3179) and eIF2α (9721) and dephosphorylated form of eIF2α (9722) were from Cell Signaling Technology. The rabbit antiserum against CNX was generated as described previously (Danilczyk and Williams, 2001), the antibody against PERK (H300) and against GADD45 were from Santa Cruz and the rabbit antiserum against PDI (SPA-891) was from StressGen Biotechnologies. Caspase-8 was detected by using a human (mAB 9746) and a mouse-specific (4927) antibody from Cell Signaling Technology. The mouse monoclonal antibodies specific for actin and glyceraldehyde 3-phosphate dehydrogenase (MAB374) were from AbCys SA and Millipore, respectively. The rabbit polyclonal antibodies for BIP (IMG-5228A) and the rat monoclonal antibody specific for GRP94 (MA3-016) were purchased from Imgenex (San Diego, CA) and ABR, respectively. Rabbit anti-ERp57 antibodies were described previously (Zhang *et al*, 2006) and mAb 12CA5 specific for influenza HA was provided by Dr Tania Watts, University of Toronto. Phalloidin, Hoechst 33342 and CMTMROS were from Molecular Probes (Invitrogen). The antibody against activated Bax

(6A7) was from BD Pharmingen and activated Bak (Ab-1) from Calbiochem. *N*-Acetyl-L-cysteine (NAC) and reduced L-glutathione (GSH) were purchased from Sigma-Aldrich. NAC and GSH were prepared at 5 mM extemporarily in complete media followed by pH adjustment to pH 7.3–7.4. Brefeldin A (Calbiochem) was used at 10 μM, whereas latrunculin B and nocodazole (Sigma-Aldrich) were used at 5 nM and 100 nM, respectively. The recombinant human Apo2L/TRAIL was purchased from Axxora platform (Alexis Corporation, Switzerland).

Cells, transfection and treatments

CT26 cells were cultured in RPMI 1640 medium, HeLa cells and MEF in DMEM medium and HCT116 cells in McCoys 5A medium (Gibco BRL). All media were supplemented by heat-inactivated FBS, 10 mM HEPES, 100 U/ml penicillin and 100 μg/ml streptomycin. CT26 cells were transfected with siRNA heteroduplexes specific for human PERK (5′-CTCACAGGCAAAGGAAGGAG-3′), mouse PERK-1 (5′-UAGAGGAGUUCAAACAGAAUCAAGC-3′), mouse PERK-2 (5′-UCUUUGAACCAUCAUAUGCUCUUGGG-3′), PKR (5′-CGUUGCUUAUGAAUGGUCUU-3′), mouse ATF6 smart pool (Dharmacon), Bak (Hs_BAK1_5) and Bax (Hs_BAX_10), SNAP23 (5′-GAGGCAGAGAAGACUUUAA-3′), VAMP-1 (5′-GGACAUCAUGC GUGUGAAU-3′) and SNAP25 (5′-CAGGCAUUGCACUAAAAGU-3′) at a final concentration of 100 nM using HiPerFect (Qiagen) according to the manufacturer's instructions. At 48 h after transfection, CT26 cells were assessed for total content of the respective proteins by immunoblotting.

HeLa cells, 1×10^5 cells per well, were seeded into 12-well plates and transfected 24 h later with either an empty vector or a vector expressing the caspase-resistant Bap31 mutant (crBAP31–Flag) (Nguyen *et al*, 2000) by using Lipofectamine™ 2000 (Gibco BRL) according to the manufacturer's instructions. The induced expression of the mutant was validated by probing with an anti-Flag antibody (data not shown). Here, 1 μM MTX, 30 μM OXP and 100 J/cm^2 UVC were the concentrations of the agents used to treat the cells for 4 h unless otherwise indicated. Z-VAD-fmk was used at 50 μM. Biotinylated VAD-fmk (bVAD-fmk) was used at 50 μM and purchased from Calbiochem.

Plasmid construction

For construction of shRNAs, self-annealing oligonucleotides containing inverted repeats separated by a spacer sequence were synthesized. Oligos were cloned into the pSuppressorRetro vector (Imgenex), which carries the U6 gene promoter and allows the expression of shRNA. A scrambled sequence provided by the kit was used as a control (shCO). shRNA plasmids were then transfected, along with packaging vectors gag-pol and vsv-g, into HEK293T cells, and retroviral supernatants were concentrated by centrifugation, as described in the manufacturer's instructions.

Caspase-8 shRNA (21 nt target underlined). 1-2 sense oligo: 5′-TCGAGCTCTTCTACCTCTTGATAGACTCCTGTATCAAGAGGTAGAA GAGCTTTTT-3′; 2-1 sense oligo: 5′-TCGAGCAACAGAACCACACTTTA GACTCCTGTAAAGTGTGGTTCTGTTGCTTTTT-3′.

PERK shRNA (21 nt target underlined). 9-2 sense oligo: 5′-TCGAGCGGCAGGTCCTTGGTAATGACTCCTGATTACCAAGGACCTGCC GCTTTTT-3′; 10-3: 5′-TCGACCAGGCATTGTGAGGTATTGACTCCTGAA-TACCTCACAATGCCTGGTTTTT-3′; 11-13: 5′-TCGAGCGGCAACGCGT CCAGTAAGACTCCTGTTACTGGACGCGTTGCCGCTTTTT-3′.

Generation of shRNA stable cell clones

For generation of stable PERK and caspase-8 shRNA-expressing cell clones, CT26 cells were infected with retroviral particles carrying the PERK, caspase-8 or scrambled shRNA plasmids, and several clones were isolated following selection in geneticin (0.1 mg/ml) for 10 days. Knockdown of PERK and caspase-8 was confirmed by western blotting.

Activated caspase detection by precipitation with bVAD-fmk

This assay was performed as previously described (Tu *et al*, 2006). Briefly, HeLa cells were incubated with 50 μM bVAD-fmk (ICN Pharmaceuticals, Irvine, CA) or DMSO control for 1 h at 37 °C. Cells were then treated for the indicated time points with 1 μM MTX and lysed in 500 μl CHAPS lysis buffer (150 mM KCl, 50 mM HEPES, 0.1% CHAPS, at pH 7.4), centrifuged at 15 000 *g* for 10 min, and the supernatants boiled for 5 min. Streptavidin-agarose (30 μl) was then added to the supernatants and agitated at 4 °C overnight, after which lysates were precipitated, washed and resolved by SDS–PAGE. Caspases were detected by immunoblotting. The endogenously biotinylated protein acetyl-CoA carboxylase was detected as a loading control.

Flow cytometric analysis of cell surface proteins

Here, 2×10^5 cells were plated in 12-well plates and the next day the cells were treated with the indicated agents for 4 h. Cells were harvested, washed twice with PBS and fixed in 0.25% paraformaldehyde (PFA) in PBS for 5 min. After washing again twice in cold PBS, cells were incubated for 30 min with primary antibody, diluted in cold blocking buffer (2% FBS in PBS), followed by washing and incubation with the FITC-conjugated monoclonal or polyclonal secondary antibody in blocking buffer (30 min). Each sample was then analysed by FACScan (Becton Dickinson) to identify cell surface CRT and ERp57. Isotype-matched IgG antibodies or second antibody alone were used as a control, and the fluorescent intensity of stained cells was gated on propidium iodide (PI)- or 4,6-diamidino-2-phenylindole (DAPI)-negative cells.

Immunofluorescence

For surface detection of ER proteins, cells were placed on ice, washed twice with PBS and fixed in 0.25% PFA in PBS for 5 min. Cells were then washed twice in PBS, and primary antibody, diluted in cold blocking buffer, was added for 30 min. After three washes in cold PBS, cells were incubated for 30 min with the appropriate secondary antibody diluted in cold blocking buffer. Cells were washed with PBS and mounted on slides with the mounting medium, including DAPI from Vectashield. For intracellular staining, cells were washed with PBS, fixed with 4% PFA for 20 min, permeabilized with 0.1% Triton X-100 for 10 min, rinsed three times with PBS, and nonspecific binding sites were blocked with 10% FBS in PBS for 30 min. Primary antibody was added for 1 h. Subsequently, cells were washed three times with PBS and incubated for 30 min in Alexa Fluor FITC or 568-conjugated secondary antibodies (1:1000; Molecular Probes). For MOMP analysis, cells were incubated with 150 nM CMTMROS for 30 min followed by CRT surface staining.

Assessment of apoptosis

Plasma membrane phosphatidylserine exposure is a marker of apoptosis and was assessed by annexin fluorescein isothiocyanate (MACS, Miltenyi Biotech) (Zamzami *et al*, 2000; Castedo *et al*, 2002). Here, 2×10^5 cells per sample were collected, washed in PBS, pelleted and resuspended in incubation buffer (10 mM HEPES/NaOH, pH 7.4, 140 mM NaCl and 5 mM $CaCl_2$) containing 1% annexin V and PI. Samples were kept in the dark and incubated for 15 min prior to the addition of another 400 μl of incubation buffer and subsequent analysis on a fluorescence-activated cell sorter Calibur flow cytometer (Becton Dickinson) using Cell Quest software.

Antitumour vaccination

Here, 3×10^6 CT26 cells untreated or treated either with MTX or OXP for 4 h were inoculated subcutaneously in 200 μl PBS into 6-week-old female BALB/c mice (Janvier) into the lower flank, whereas 5×10^5 untreated control cells were inoculated into the contralateral flank 7 days later (Casares *et al*, 2005). To restore ecto-CRT, CT26 cells were incubated with recCRT, produced in insect cells (Obeid *et al*, 2007c), at 3 μg/10^6 cells in PBS on ice for 30 min, followed by three washes. Animals bearing tumours in excess of 20–25% of the body mass were killed. All animals were maintained in specific pathogen-free conditions, and all experiments followed the Federation of European Laboratory Animal Science Association guidelines. All animal experiments were approved by the Ethical Committee of Institut Goustave Roussy (IGR).

Supplementary data

Supplementary data are available at *The EMBO Journal* Online (http://www.embojournal.org).

Acknowledgements

We thank Drs Richard Flavell (Yale University, NH), Bert Vogelstein (John Hopkins University, Bethesda, ML), Randal Kaufman (University of Michigan Medical Center, Ann Arbor, MI) and

David Wallach (Weizmann Insitute, Rehovot, Israel) for knockout or knock-in cell lines, Victor Goldmacher (ImmunoGen, Cambridge, MA) for HeLa transfectants, and Gordon Shore (McGill University, Montreal, Canada) for Bap31 mutants. We also thank Hideo Yagita for TRAIL antibody, Steven Doyle for help with confocal microscopy and Myrna Cohen-Doyle for help with pulse-chase experiments. GK is supported by the Ligue Nationale contre le Cancer (Equipe labellisée), European Commission (active p53, Apo-Sys, RIGHT, TransDeath, ChemoRes, DeathTrain), Cancéropôle Ile-de-France, Fondation de France and Fondation pour la Recherche Médicale; TP is supported by the Swedish Research Council (Vetenskapsrådet); AT is supported by Poste d'accueil INSERM; OK is supported by EMBO; UB is supported by the CIHR Training Program in the Structural Biology of Membrane Proteins Linked to Disease and by operating grants to DBW from the CIHR and Canadian Cancer Society, MD by the Fonds zur Förderung der wissenschaftlichen Forschung (Austria) for grant 'Molecular Enzymology', FM by the Fonds zur Förderung der wissenschaftlichen Forschung (Austria), grant S-9304-B05.

References

Afshar N, Black BE, Paschal BM (2005) Retrotranslocation of the chaperone calreticulin from the endoplasmic reticulum lumen to the cytosol. *Mol Cell Biol* **25:** 8844–8853

Apetoh L, Ghiringhelli F, Tesniere A, Obeid M, Ortiz C, Criollo A, Mignot G, Maiuri MC, Ullrich E, Saulnier P, Yang H, Amigorena S, Ryffel B, Barrat FJ, Saftig P, Levi F, Lidereau R, Nogues C, Mira JP, Chompret A *et al* (2007) Toll-like receptor 4-dependent contribution of the immune system to anticancer chemotherapy and radiotherapy. *Nat Med* **13:** 1050–1059

Bedard K, Szabo E, Michalak M, Opas M (2005) Cellular functions of endoplasmic reticulum chaperones calreticulin, calnexin, and ERp57. *Int Rev Cytol* **245:** 91–121

Ben Moshe T, Barash H, Kang TB, Kim JC, Kovalenko A, Gross E, Schuchmann M, Abramovitch R, Galun E, Wallach D (2007) Role of caspase-8 in hepatocyte response to infection and injury in mice. *Hepatology* **45:** 1014–1024

Black S, Kadyrov M, Kaufmann P, Ugele B, Emans N, Huppertz B (2004) Syncytial fusion of human trophoblast depends on caspase 8. *Cell Death Differ* **11:** 90–98

Breckenridge DG, Stojanovic M, Marcellus RC, Shore GC (2003) Caspase cleavage product of BAP31 induces mitochondrial fission through endoplasmic reticulum calcium signals, enhancing cytochrome *c* release to the cytosol. *J Cell Biol* **160:** 1115–1127

Casares N, Pequignot MO, Tesniere A, Ghiringhelli F, Roux S, Chaput N, Schmitt E, Hamai A, Hervas-Stubbs S, Obeid M, Coutant F, Metivier D, Pichard E, Aucouturier P, Pierron G, Garrido C, Zitvogel L, Kroemer G (2005) Caspase-dependent immunogenicity of doxorubicin-induced tumor cell death. *J Exp Med* **202:** 1691–1701

Castedo M, Ferri K, Roumier T, Metivier D, Zamzami N, Kroemer G (2002) Quantitation of mitochondrial alterations associated with apoptosis. *J Immunol Methods* **265:** 39–47

Charruyer A, Grazide S, Bezombes C, Muller S, Laurent G, Jaffrezou JP (2005) UV-C light induces raft-associated acid sphingomyelinase and JNK activation and translocation independently on a nuclear signal. *J Biol Chem* **280:** 19196–19204

Danilczyk UG, Williams DB (2001) The lectin chaperone calnexin utilizes polypeptide-based interactions to associate with many of its substrates *in vivo*. *J Biol Chem* **276:** 25532–25540

Ellgaard L, Riek R, Herrmann T, Guntert P, Braun D, Helenius A, Wuthrich K (2001) NMR structure of the calreticulin P-domain. *Proc Natl Acad Sci USA* **98:** 3133–3138

Ferro-Novick S, Jahn R (1994) Vesicle fusion from yeast to man. *Nature* **370:** 191–193

Franz S, Herrmann K, Furnrohr BG, Sheriff A, Frey B, Gaipl US, Voll RE, Kalden JR, Jack HM, Herrmann M (2008) After shrinkage apoptotic cells expose internal membrane-derived epitopes on their plasma membranes. *Cell Death Differ* **15:** 805

Goldmacher VS, Bartle LM, Skaletskaya A, Dionne CA, Kedersha NL, Vater CA, Han JW, Lutz RJ, Watanabe S, Cahir McFarland ED, Kieff ED, Mocarski ES, Chittenden T (1999) A cytomegalovirus-encoded mitochondria-localized inhibitor of apoptosis structurally unrelated to Bcl-2. *Proc Natl Acad Sci USA* **96:** 12536–12541

Harding HP, Zhang Y, Bertolotti A, Zeng H, Ron D (2000) Perk is essential for translational regulation and cell survival during the unfolded protein response. *Mol Cell* **5:** 897–904

Kang TB, Ben-Moshe T, Varfolomeev EE, Pewzner-Jung Y, Yogev N, Jurewicz A, Waisman A, Brenner O, Haffner R, Gustafsson E, Ramakrishnan P, Lapidot T, Wallach D (2004) Caspase-8 serves both apoptotic and nonapoptotic roles. *J Immunol* **173:** 2976–2984

Kapoor M, Srinivas H, Kandiah E, Gemma E, Ellgaard L, Oscarson S, Helenius A, Surolia A (2003) Interactions of substrate with calreticulin, an endoplasmic reticulum chaperone. *J Biol Chem* **278:** 6194–6200

Kaufman RJ (1999) Stress signaling from the lumen of the endoplasmic reticulum: coordination of gene transcriptional and translational controls. *Genes Dev* **13:** 1211–1233

Laurent A, Nicco C, Chereau C, Goulvestre C, Alexandre J, Alves A, Levy E, Goldwasser F, Panis Y, Soubrane O, Weill B, Batteux F (2005) Controlling tumor growth by modulating endogenous production of reactive oxygen species. *Cancer Res* **65:** 948–956

Leach MR, Cohen-Doyle MF, Thomas DY, Williams DB (2002) Localization of the lectin, ERp57 binding, and polypeptide binding sites of calnexin and calreticulin. *J Biol Chem* **277:** 29686–29697

Lippincott-Schwartz J, Yuan LC, Bonifacino JS, Klausner RD (1989) Rapid redistribution of Golgi proteins into the ER in cells treated with brefeldin A: evidence for membrane cycling from Golgi to ER. *Cell* **56:** 801–813

Nakagawa T, Zhu H, Morishima N, Li E, Xu J, Yankner BA, Yuan J (2000) Caspase-12 mediates endoplasmic-reticulum-specific apoptosis and cytotoxicity by amyloid-beta. *Nature* **403:** 98–103

Ng FW, Nguyen M, Kwan T, Branton PE, Nicholson DW, Cromlish JA, Shore GC (1997) p28 Bap31, a Bcl-2/Bcl-XL- and procaspase-8-associated protein in the endoplasmic reticulum. *J Cell Biol* **139:** 327–338

Nguyen M, Breckenridge DG, Ducret A, Shore GC (2000) Caspase-resistant BAP31 inhibits fas-mediated apoptotic membrane fragmentation and release of cytochrome *c* from mitochondria. *Mol Cell Biol* **20:** 6731–6740

Novoa I, Zeng H, Harding HP, Ron D (2001) Feedback inhibition of the unfolded protein response by GADD34-mediated dephosphorylation of eIF2alpha. *J Cell Biol* **153:** 1011–1022

Obeid M, Panaretakis T, Joza N, Tufi R, Tesniere A, van Endert P, Zitvogel L, Kroemer G (2007a) Calreticulin exposure is required for the immunogenicity of gamma-irradiation and UVC light-induced apoptosis. *Cell Death Differ* **14:** 1848–1850

Obeid M, Panaretakis T, Tesniere A, Joza N, Tufi R, Apetoh L, Ghiringhelli F, Zitvogel L, Kroemer G (2007b) Leveraging the immune system during chemotherapy: moving calreticulin to the cell surface converts apoptotic death from 'silent' to immunogenic. *Cancer Res* **67:** 7941–7944

Obeid M, Tesniere A, Ghiringhelli F, Fimia GM, Apetoh L, Perfettini JL, Castedo M, Mignot G, Panaretakis T, Casares N, Metivier D, Larochette N, van Endert P, Ciccosanti F, Piacentini M, Zitvogel L, Kroemer G (2007c) Calreticulin exposure dictates the immunogenicity of cancer cell death. *Nat Med* **13:** 54–61

Panaretakis T, Joza N, Modjtahedi N, Tesniere A, Vitale I, Durchschlag M, Fimia GM, Kepp O, Piacentini M, Froehlich KU, van Endert P, Zitvogel L, Madeo F, Kroemer G (2008) The co-translocation of ERp57 and calreticulin determines the immunogenicity of cell death. *Cell Death Differ* **15:** 1499–1509

Pauleau AL, Larochette N, Giordanetto F, Scholz SR, Poncet D, Zamzami N, Goldmacher VS, Kroemer G (2007) Structure–function analysis of the interaction between Bax and the cytomegalovirus-encoded protein vMIA. *Oncogene* **26:** 7067–7080

Rothman JE, Sollner TH (1997) Throttles and dampers: controlling the engine of membrane fusion. *Science* **276:** 1212–1213

Schrag JD, Bergeron JJ, Li Y, Borisova S, Hahn M, Thomas DY, Cygler M (2001) The structure of calnexin, an ER chaperone involved in quality control of protein folding. *Mol Cell* **8:** 633–644

Schroder M, Kaufman RJ (2005) The mammalian unfolded protein response. *Annu Rev Biochem* **74:** 739–789

Scorrano L, Oakes SA, Opferman JT, Cheng EH, Sorcinelli MD, Pozzan T, Korsmeyer SJ (2003) BAX and BAK regulation of endoplasmic reticulum Ca^{2+}: a control point for apoptosis. *Science* **300:** 135–139

Tu S, McStay GP, Boucher LM, Mak T, Beere HM, Green DR (2006) *In situ* trapping of activated initiator caspases reveals a role for caspase-2 in heat shock-induced apoptosis. *Nat Cell Biol* **8:** 72–77

Tufi R, Panaretakis T, Bianchi K, Criollo A, Fazi B, Di Sano F, Tesniere A, Kepp O, Paterlini-Brechot P, Zitvogel L, Piacentini M, Szabadkai G, Kroemer G (2008) Reduction of endoplasmic reticulum Ca^{2+} levels favors plasma membrane surface exposure of calreticulin. *Cell Death Differ* **15:** 274–282

Valentijn JA, Valentijn K, Pastore LM, Jamieson JD (2000) Actin coating of secretory granules during regulated exocytosis correlates with the release of rab3D. *Proc Natl Acad Sci USA* **97:** 1091–1095

Valentijn K, Valentijn JA, Jamieson JD (1999) Role of actin in regulated exocytosis and compensatory membrane retrieval: insights from an old acquaintance. *Biochem Biophys Res Commun* **266:** 652–661

Vibet S, Maheo K, Gore J, Dubois P, Bougnoux P, Chourpa I (2007) Differential subcellular distribution of mitoxantrone in relation to chemosensitization in two human breast cancer cell lines. *Drug Metab Dispos* **35:** 822–828

Zamzami N, El Hamel C, Maisse C, Brenner C, Munoz-Pinedo C, Belzacq AS, Costantini P, Vieira H, Loeffler M, Molle G, Kroemer G (2000) Bid acts on the permeability transition pore complex to induce apoptosis. *Oncogene* **19:** 6342–6350

Zhang Y, Baig E, Williams DB (2006) Functions of ERp57 in the folding and assembly of major histocompatibility complex class I molecules. *J Biol Chem* **281:** 14622–14631

